Electronic Supplementary Material (ESI) for Nanoscale.

Electronic Supporting Information

Thermally Reduced Fluorographenes as Efficient Electrode Materials for Supercapacitors

Martin Petr[a], Petr Jakubec[b], Václav Ranc[b], Veronika Šedajová[b], Rostislav Langer[b], Miroslav Medveď[b], Piotr Błoński[b], Josef Kašlík[b], Vojtěch Kupka[b], Michal Otyepka[b]* and Radek Zbořil[b]*

Msc. M. Petr, Dr. P. Jakubec, Dr. V. Ranc, Msc. Veronika Šedajová, MSc. R. Langer, Dr. M. Medveď, Dr. P. Błoński, Dr. J. Kašlík, Dr. V. Kupka, Prof. Dr. M. Otyepka, Prof. Dr. R. Zbořil,

[a]Regional Centre for Advanced Technologies and Materials, Department of Experimental Physics, Faculty of Science, Palacký University Olomouc, 17. listopadu 1192/12, 771 46 Olomouc, Czech Republic

[b]Regional Centre for Advanced Technologies and Materials, Department of Physical Chemistry, Faculty of Science, Palacký University Olomouc, 17. listopadu 1192/12, 771 46 Olomouc, Czech Republic

E-mail: p.jakubec@upol.cz, michal.otyepka@upol.cz

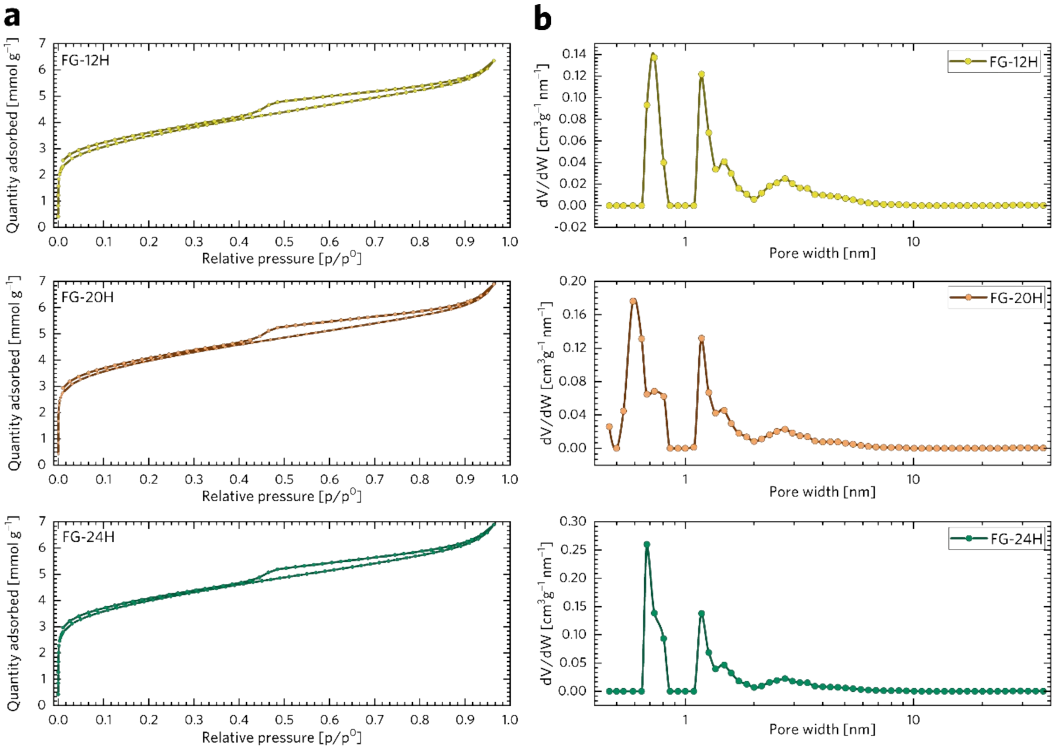

Figure S1 | (a) Nitrogen adsorption–desorption isotherms of FG-12H, FG-20H and FG-24H samples and (b) pore size distribution curve above mentioned samples

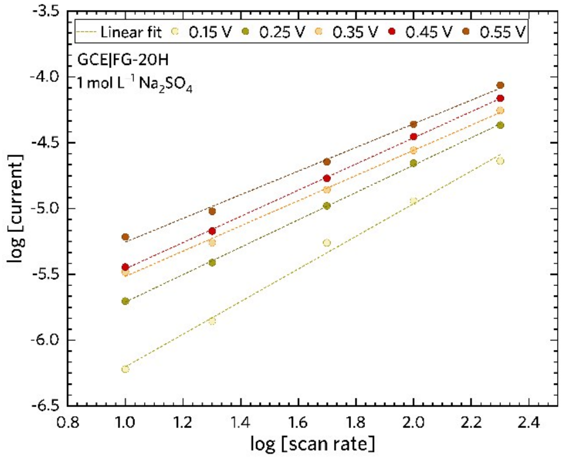

Figure S2 | The plot of log *i* vs. log *v* of FG-20H sample.

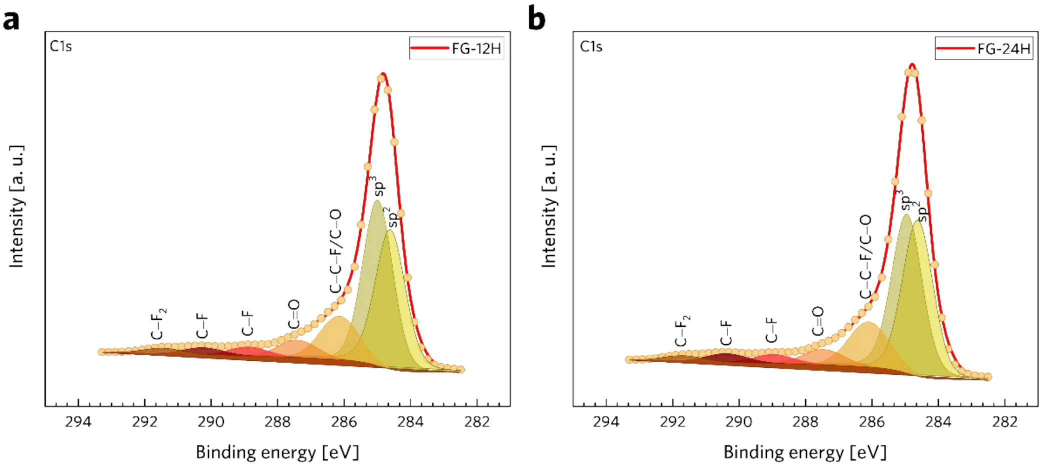

Figure S3 | HR-XPS spectra of C1s derived from FG-12H and FG-24H sample

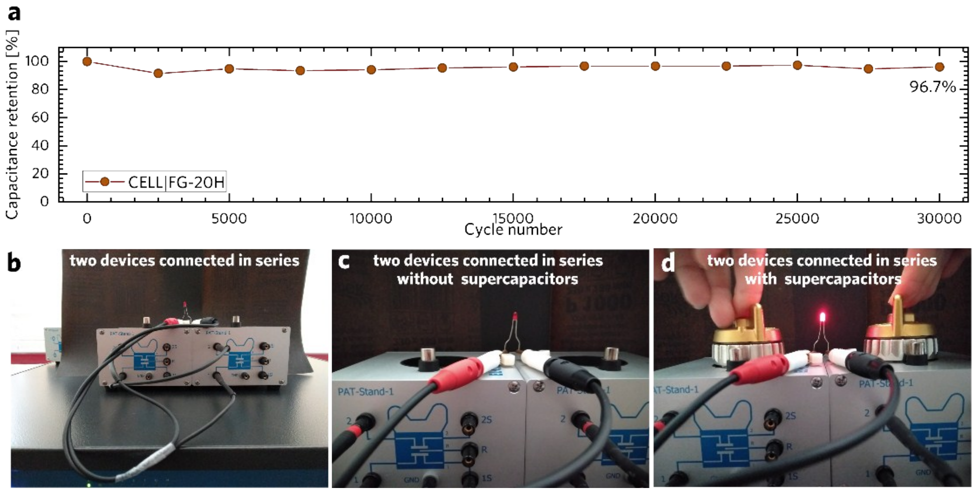

Figure S4 | (a) cyclic stability (30 000 cycles) of FG-20H sample in two-electrode setup. (b, c) two devices connected in series. (d) two devices connected in series powered red LED diode

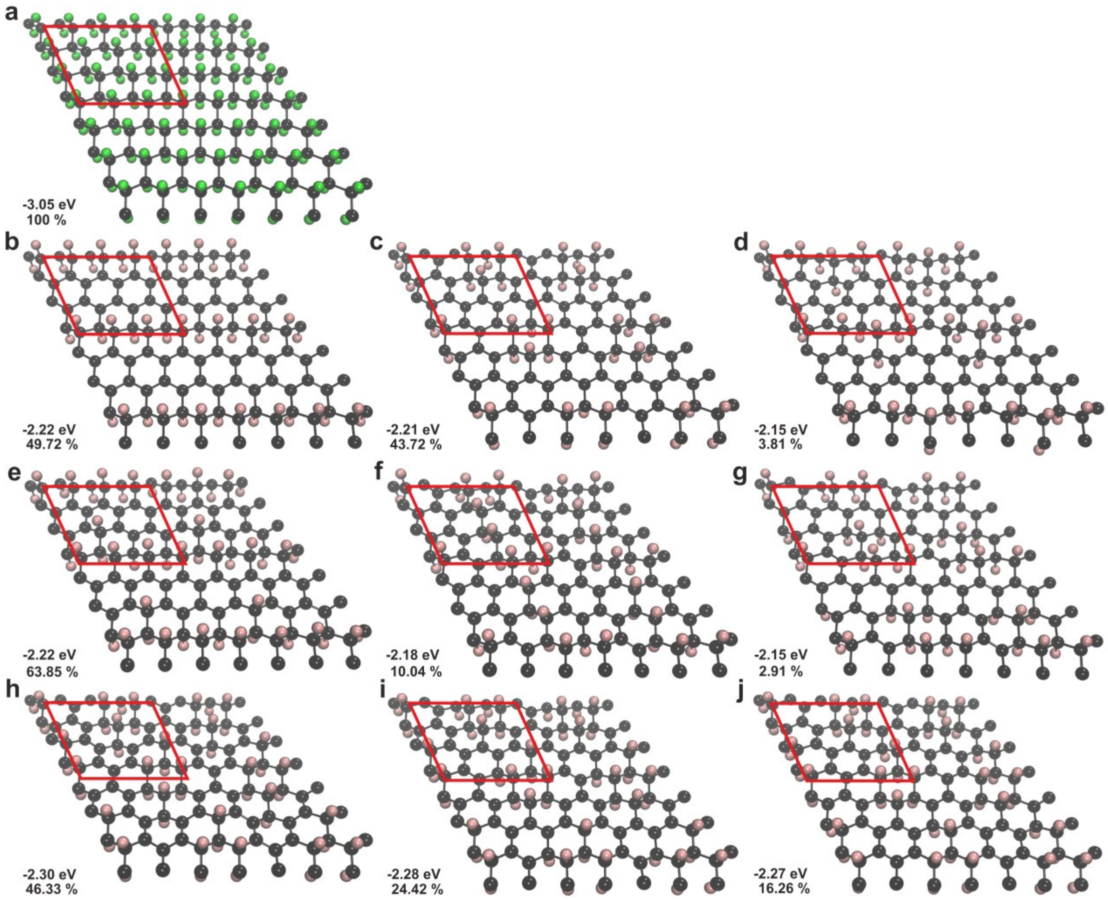

Figure S5 | (a) fully fluorinated graphene, and partially hydrogenated graphene: (b-d) $C_{18}H_6$, (e-g) $C_{18}H_7$ and (h-j) $C_{18}H_8$. The numbers refer to binding energy [eV] and Boltzmann probability [%] of occurrence at a certain arrangement. Red frames depict the unit cell.

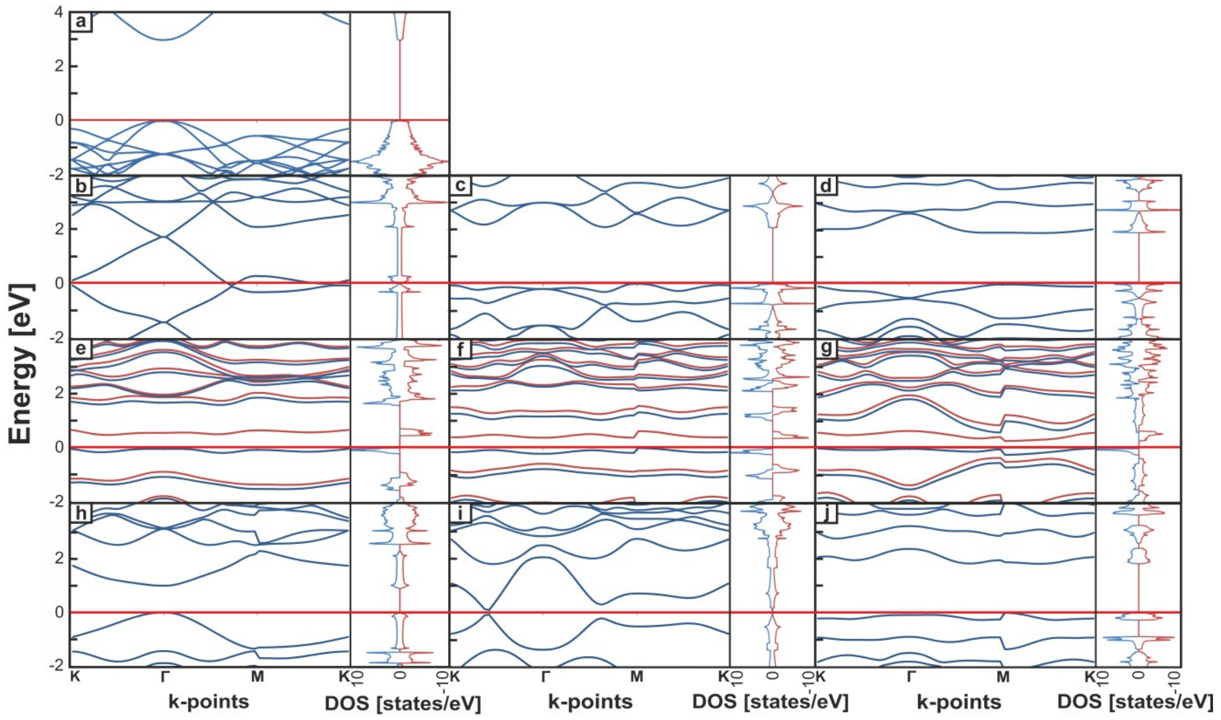

Figure S6 | Density of states and band structure of (a) fully fluorinated graphene, and (b-j) partially hydrogenated graphene. The electronic structure is influenced by different stoichiometry and topology of hydrogen ad-atoms. The labeling of individual panels corresponds to the structures depicted in Figure S4.

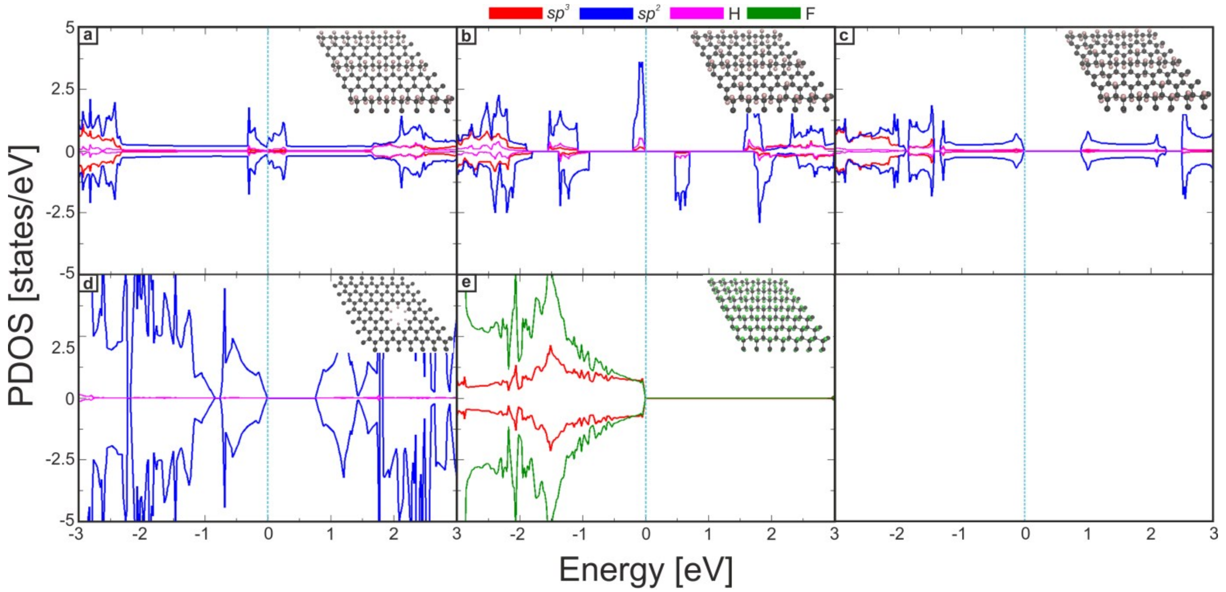

Figure S7 | Projected density of states of (a-c) partially hydrogenated graphene ($C_{18}H_6$, $C_{18}H_7$, and $C_{18}H_8$), (d) partially hydrogenated graphene after fragmentation ($C_{66}H_6$), and (e) fully fluorinated graphene.

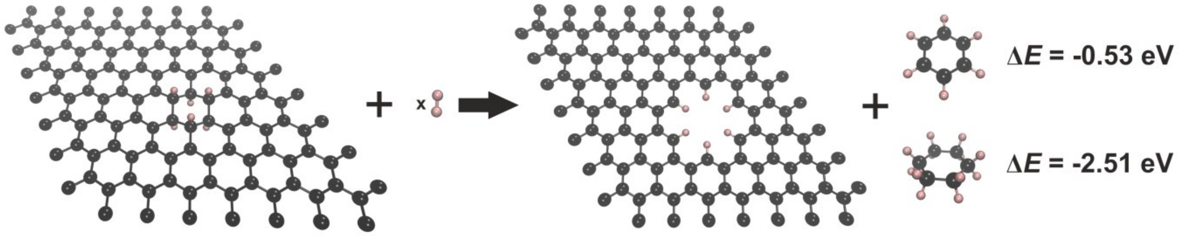

Figure S8 | Feasibility of the fragmentation in the final phase is demonstrated by negative reaction energies for the release of C_6H_6 and C_6H_{12} fragments.

Analysis of the band structure in heavily defluorinated FG

To address a possible relation of the content and topology of F ad-atoms with the observed changes in the electrochemical properties of heavily defluorinated samples, the electronic structure of various FG motifs was computed following the mechanism the mechanism displayed in Scheme S1. The defluorination phase leading to various low fluorine content structures (due to high temperature conditions) is followed by a reorganization (aggregation) phase, in which fluorine ad-atoms migrate over the lattice, forming small aggregates, which perhapsslightly modify the size of sp^2 carbon atom domains. However, the sp^2/sp^3 ratio is practically kept constant. In the final phase, the aggregates are released from the lattice as molecular fragments, thus increasing the material porosity and the number of sp^3 carbon atoms at the edges. The band gaps and density of states for selected $C_{48}F_2$ structures corresponding to the fluorine content of 4 % shown in Fig. S9-S10 indicate that the structures can be metallic or semiconducting, depending on the position of fluorine ad-atoms. The reorganization of ad-atoms indeed affects the electric properties of the material, and, therefore, they can also partly explain the monotonous increase in the specific capacitance in phase 2. In addition, the barriers for migration of fluorine ad-atoms were found to be rather low, following the top-bridge-top barrier of 0.34 eV for a single fluorine ad-atom and of 0.87–1.05 eV for the formation of a pair of F ad-atoms on the neighboring carbon atoms in double-sided functionalized graphene, while the reverse process (the breaking of the pair) requires higher energy (1.6 eV), which is in agreement with literature[S1]. The barrier heights thus favor the aggregation of F adatoms. However, it should be noted that the very low content of ad-atoms is in contradiction with relatively high proportion of sp^3 carbon atoms in our samples (see Fig. 3 and S3). In conclusion, although the observed changes in the electric properties could be partly attributed to the changes in the content and topology of F ad-atoms, they do not satisfactorily explain the changes inthe ratio of the sp^3/sp^2 carbon atoms.

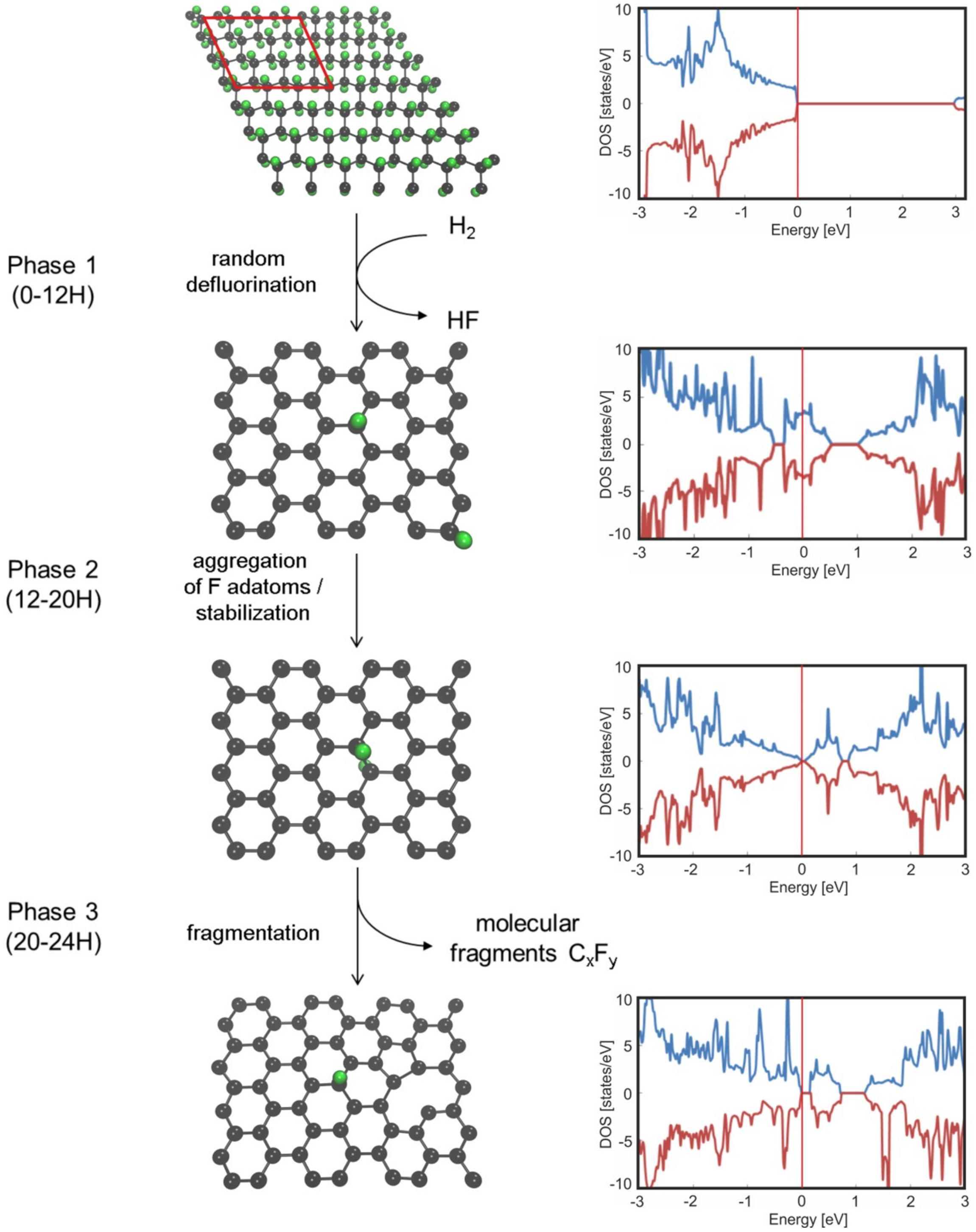

Scheme S1 | An alternative mechanism of defluorination of fluorographene under the reducing hydrogen atmosphere. The Fermi level in DOS (states/eV per computational cell) is set to zero.

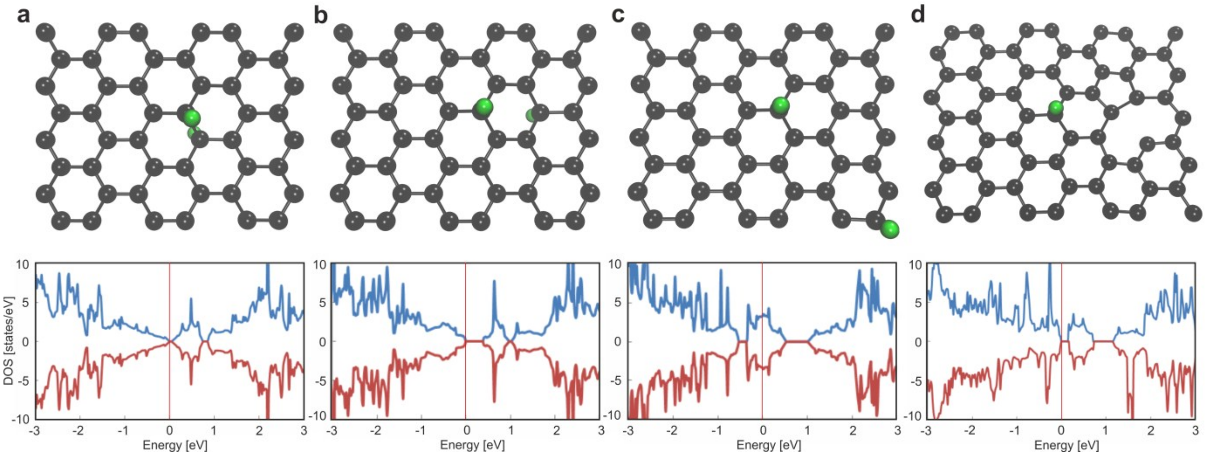

Figure S9 | Density of states of (a-c) partially fluorinated graphene ($C_{48}F_2$) and (d) defected partially fluorinated graphene ($C_{47}F_1$). The electronic structure is influenced by the arrangement of the fluorine ad-atoms.

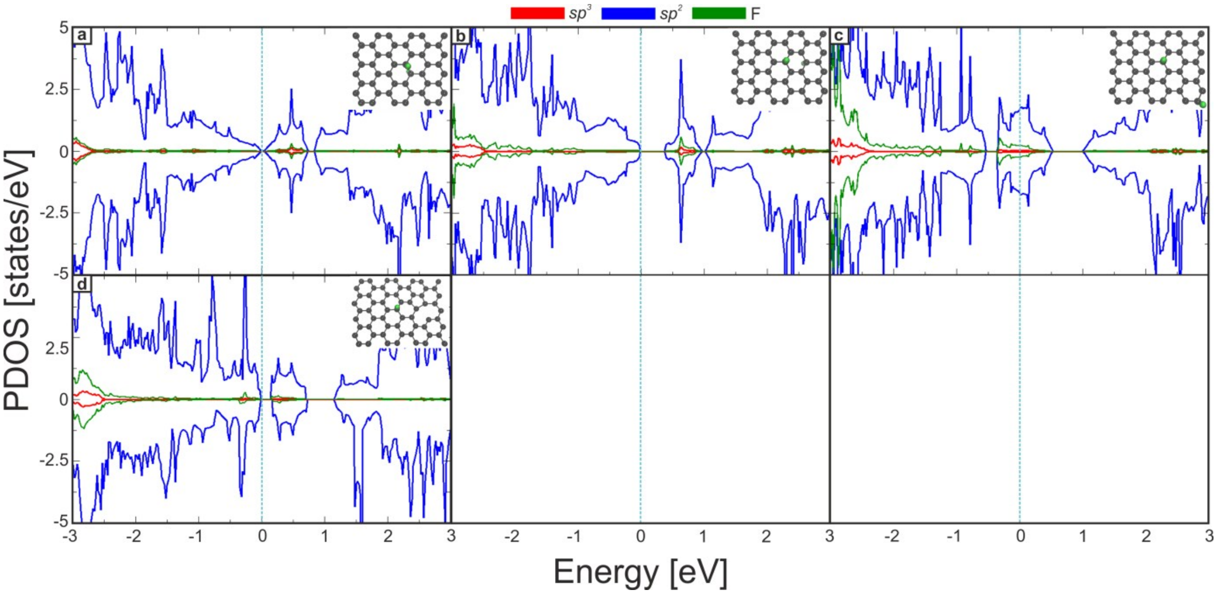

Figure S10 | Projected density of states of (a-c) partially fluorinated graphene ($C_{48}F_2$) with different arrangement of F ad-atoms, (d) defected partially fluorinated graphene ($C_{47}F_1$).

References

S1 A. Zhimin, Q. Jiang, S. Li, H. Liu, F. M. Peeters, S. Li and G. Wang, *ACS Applied Materials & Interfaces* 2015, ***7***, 19659–19665.